Optical and Quantum Electronics **34:** 217–226, 2002.

The photonic analogue of the graded heterostructure: Analysis using the envelope approximation

EMANUEL ISTRATE* AND EDWARD H. SARGENT
Department of Electrical and Computer Engineering, University of Toronto, 10 King's College Road, Toronto, Ontario, Canada M5S 3G4
*(*author for correspondence: E-mail: e.istrate@utoronto.ca)*

Abstract. We develop and deploy an envelope function formalism in order to study graded photonic crystals – periodic photonic media whose features vary continuously with position. We use the method to reduce the properties of the uniform crystals to the spectral position of their band edges and an effective mass-like term. These are employed within the Schrödinger-like equation derived herein to determine the behaviour of light inside a specific graded photonic crystal created using depth-dependent infiltration of an artificial opal.

Key words: approximation methods, chirped gratings, graded junctions, heterostructures, photonic crystals

1. Introduction

The analogy between wave behaviour in electronic and photonic crystals has proven instructive, inspirational, and imperfect.

Much less explored to date is an analogy in photonics with the revolution in electronics enabled by demonstration of heteroepitaxial fabrication methods. The concatenation of electronic crystals – be they lattice-matched, strained, or dislocated – has led to the embodiment of complex functionality inside a single electronic device. Electronic functional devices exploit engineering of the quantum mechanical behaviour of charge carriers through controlled variation of the local band structure. Resonant tunnelling diodes and transistors, in which high speed, negative differential resistance, and multistable memory functions are exhibited, epitomize this principle of transforming novel physics into useful function.

One important aspect of electronic band structure engineering is the realization of graded heterostructures, in which the composition is varied continuously in space. Electronic and optoelectronic devices which exploit these effects include, to date: graded-base heterostructure bipolar transistors which promote the egress of carriers through the base; graded separate confinement heterostructure laser active regions which not only confine light to the quantum wells, but may also promote transport within the active region and increase device bandwidth (Marcinkevicius *et al.* 1995); graded

p–n junction solar cells with increased conversion efficiency (Sinkkonen 1994); superlattice graded band gap photodiodes with increased bandwidth (Yih *et al.* 1995); delta-doped graded heterostructures in which regions of doping are separated from regions of conduction for reduced carrier scattering (Li *et al.* 1999).

The importance of semiconductor compositional grading extends beyond the realm of deliberate band structure engineering. Real bulk crystals exhibit slowly varying strain fluctuations across their spatial extent. Amorphous semiconductors may employ spatially varying densities of states (Furlan *et al.* 1993). Ohmic contact formation between metallic alloys and semiconductors has been described in terms of effective band structure grading (Wuyts *et al.* 1992).

Thus, compositional grading is of critical importance to the operation and understanding of contemporary electronics. Its importance extends from functionally complex band structure-engineered devices to simple material interfaces and even nominally bulk media.

In response, we have adopted the view that analogous phenomena in photonic crystals may be of similar importance in transforming the novel physics of the photonic band gap into useful, novel function.

Photonic crystal heterostructures have been recently introduced as a means to create functional devices using photonic crystals (Istrate and Sargent 2000a, E. Istrate and E. H. Sargent, submitted; Yano *et al.* 2000). The analysis and simulation of such photonic structures is more difficult than that of uniform, or bulk, photonic crystals, due to the fact that the infinite periodicity of the sample may no longer be exploited. An alternative method for the analytical computation of the behaviour of such structures was proposed (E. Istrate and E. H. Sargent, submitted), which simplifies this problem significantly.

Graded – or chirped – photonic crystals are a special case of a photonic crystal junction, where the properties of the crystal vary smoothly over a significant number of photonic crystal layers, as compared to the abrupt variation of the heterostructures discussed so far. They can appear accidentally in the fabrication of photonic crystals by infiltration (Blanco *et al.* 2000) if the infiltration process is not completely uniform over the entire volume of the sample. Different levels of infiltration translate into different average refractive indices and hence different band structures. Graded structures can also appear during the holographic fabrication of photonic crystals by interference of four laser beams (Campbell *et al.* 2000). In such a structure attenuation of the beams as they traverse the photoresist may produce a non-uniform, graded sample. A good understanding of the behaviour of graded photonic crystals is therefore essential when evaluating the quality of infiltrated photonic crystals as well as for crystals produced holographically.

In this paper the use of the envelope approximation (E. Istrate and E. H. Sargent, submitted) with graded, slowly varying, photonic crystals is discussed. The work is analogous with the analysis of semiconductor electronic heterostructures and graded junctions (Weisbuch and Vinter 1991; Chow and Koch 1999).

2. Theory

A graded photonic crystal junction, like any photonic crystal heterostructure displays variations on two length scales. The first is the periodicity of the underlying photonic crystal, called the bulk crystal in the present work. The second variation is due to the grading of the structure and is a much slower variation. For the inverted opals with varying infiltration this could take the form of an increasing average index.

The envelope approximation presented herein separates the effects of the variations on these two scales and allows analysis to take place in two steps. First, knowledge of the band structure of the bulk crystals forming the junction is used to obtain a parameter that will describe the effects of the fast variation due to the crystal periodicity. This is similar to the effective mass used with semiconductor heterojunctions. Given knowledge of this parameter, the analysis can concentrate on the effects of the slower variation due to the graded junction. The photonic crystal is treated as a quasi-homogeneous medium described by the effective mass-like term. The approach is not unlike the successful deployment of continuous-matter approximations (e.g. hydrodynamic models) in the analysis of fundamentally discrete media composed of individual atoms.

The separation of the two length scales starts by dividing the dielectric constant of the structure into a slowly varying, a quickly varying, and a constant component:

$$\epsilon = \epsilon_b + \epsilon_s(\mathbf{r}) + \epsilon_f(\mathbf{r}) = \epsilon_b + \epsilon_v(\mathbf{r}), \tag{1}$$

where ϵ_v represents the spatially varying component of the dielectric profile. This is included in the wave equation to obtain:

$$\{\nabla^2 + \omega_\lambda^2 \mu[\epsilon_b + \epsilon_v(\mathbf{r})] - \nabla(\nabla\cdot)\}\mathbf{E}_\lambda = 0. \tag{2}$$

Here λ represents the state of the electric field in the graded junction.

Assuming that the crystal grading is much slower than the photonic crystal periodicity, we can express the electric field as a superposition of bulk Bloch modes $\mathbf{E}_{n,\mathbf{k}} = \mathbf{u}_{n,\mathbf{k}} \exp(i\mathbf{k}\cdot\mathbf{r})$. The Bloch functions can in turn be expressed

in terms of the band-edge Bloch functions $\mathbf{u}_{n,0}$, with $\mathbf{k} = 0$. Using $\langle \mathbf{u}_{m,0} | \mathbf{u}_{n,\mathbf{k}} \rangle \triangleq \langle m | n, \mathbf{k} \rangle$, we obtain:

$$\mathbf{E}_\lambda = \sum_{m,n,\mathbf{k}} \mathbf{u}_{m,0}(\mathbf{r}) \exp(i\mathbf{k} \cdot \mathbf{r}) \langle \mathbf{E}_{n,\mathbf{k}} | \mathbf{E}_\lambda \rangle \langle m | n, \mathbf{k} \rangle = \sum_{m,k} \exp(i\mathbf{k} \cdot \mathbf{r}) W_{\lambda,m,\mathbf{k}} \mathbf{u}_{m,0}(\mathbf{r}), \tag{3}$$

with $W_{\lambda,m,\mathbf{k}} \triangleq \sum_n \langle m | n, \mathbf{k} \rangle \langle \mathbf{E}_{n,\mathbf{k}} | \mathbf{E}_\lambda \rangle$. This expression for the electric field can now be used in the wave equation which takes the form:

$$\sum_{m,\mathbf{k}} W_{\lambda,m,\mathbf{k}} \{ \nabla^2 + \omega_\lambda^2 \mu [\epsilon_b + \epsilon_v(\mathbf{r})] - \nabla(\nabla \cdot) \} \exp(i\mathbf{k} \cdot \mathbf{r}) \mathbf{u}_{m,0}(\mathbf{r}) = 0. \tag{4}$$

This equation can be expanded into the form:

$$\sum_{m,\mathbf{k}} W_{\lambda,m,\mathbf{k}} \exp(i\mathbf{k} \cdot \mathbf{r}) \left[-k^2 + 2i \left(k_x \frac{\partial}{\partial x} + k_y \frac{\partial}{\partial y} + k_z \frac{\partial}{\partial z} \right) - i\nabla(\mathbf{k}\cdot) + \mathbf{k}(\mathbf{k}\cdot) \right.$$
$$\left. - i\mathbf{k}(\nabla \cdot) + (\omega_\lambda^2 - \omega_m^2)\mu\epsilon_f(\mathbf{r}) + (\omega_\lambda^2 - \omega_m^2)\mu\epsilon_b + \omega_\lambda^2 \mu \epsilon_s(\mathbf{r}) \right] \mathbf{u}_m(\mathbf{r}) = 0. \tag{5}$$

Here $\mathbf{u}_m$ represents the Bloch function $\mathbf{u}_{m,0}$ at the band edge and ω_m represents the photon frequency at this edge.

The envelope approximation separates the two length scales of the photonic crystal periodicity and of the junction variations. This is expressed mathematically by separating the position vector $\mathbf{r}$ into the two components $\mathbf{r} = \mathbf{R} + \rho$. $\mathbf{R}$ represents the position of each unit cell within the crystal, while ρ represents the positions inside the unit cell. Hence ρ is used to represent the rapid variations of the photonic crystal, while $\mathbf{R}$ is used to measure the much slower variations in the junction.

Equation (5) is solved by multiplying by $\exp(-i\mathbf{k}' \cdot \mathbf{r}) \mathbf{u}_n^*(\mathbf{r})$ and integrating over the volume of the crystal. The result, after reversing the variables $\mathbf{k}$ and $\mathbf{k}'$ is:

$$[(\omega_\lambda^2 - \omega_n^2)\mu\epsilon_b - k^2] W_{\lambda,n,\mathbf{k}} + \sum_m \left[2ik_{\pi,n,m} - i\pi_{k,n,m} + q_{n,m} - i\pi_{n,m} \right.$$
$$\left. + (\omega_\lambda^2 - \omega_m^2)\mu\epsilon_{f,n,m} \right] W_{\lambda,m,\mathbf{k}} - \sum_{\mathbf{k}'} \omega_\lambda^2 \mu \epsilon^s_{\mathbf{k}'-\mathbf{k}} W_{\lambda,n,\mathbf{k}'} = 0. \tag{6}$$

The expression above contains the approximation that ϵ_s varies slowly enough that it can be taken to be constant in each unit cell. The new terms introduced in this equation are defined as:

$$k_{\pi,n,m} \triangleq \sum_{l=x,y,z} k_l \int \mathrm{d}^3\rho \mathbf{u}_n^* \cdot \frac{\partial}{\partial l} \mathbf{u}_m, \tag{7}$$

$$\pi_{k,n,m} \triangleq \int \mathrm{d}^3\rho \mathbf{u}_n^* \cdot \nabla(\mathbf{k} \cdot \mathbf{u}_m), \tag{8}$$

$$\pi_{n,m} \triangleq \int \mathrm{d}^3\rho \mathbf{u}_n^* \cdot \mathbf{k}(\nabla \cdot \mathbf{u}_m), \tag{9}$$

$$q_{n,m} \triangleq \int \mathrm{d}^3\rho (\mathbf{u}_n^* \cdot \mathbf{k})(\mathbf{k} \cdot \mathbf{u}_m), \tag{10}$$

$$\epsilon_{f,n,m} \triangleq \int \mathrm{d}^3\rho \mathbf{u}_m^* \epsilon(\mathbf{r}) \mathbf{u}_m, \tag{11}$$

$$\epsilon^s_{\mathbf{k}-\mathbf{k}'} \triangleq \sum_{\mathbf{R}} \exp(i(\mathbf{k} - \mathbf{k}' \cdot \mathbf{R}) \epsilon_s(\mathbf{R}). \tag{12}$$

In order to compue the electric field state for a specific band, n, described by the superposition of Bloch states $W_{\lambda,n,\mathbf{k}}$, we make the approximation that all other (remote) bands $j \neq n$ do not couple with each other. We also neglect ϵ_s and $\epsilon_{f,n,m}$ for this remote band coupling and use $k^2 = \omega^2\mu\epsilon$ to approximate $k^2 \approx (\omega_\lambda - \omega_n^2)\mu\epsilon_b$ to compute the electric field state of the remote bands:

$$W_{\lambda,j,\mathbf{k}} = W_{\lambda,n,\mathbf{k}} \frac{2ik_{\pi,j,n} - i\pi_{k,j,n} + q_{j,n} - i\pi_{j,n}}{(\omega_j^2 - \omega_n^2)\mu\epsilon_b}. \tag{13}$$

This result is used for the bands $W_{\lambda,m,\mathbf{k}}$ in Equation (6):

$$W_{\lambda,n,\mathbf{k}} \Bigg\{ \left[(\omega_\lambda^2 - \omega_n^2)\mu\epsilon_b - k^2\right] + \sum_{m \neq n} \frac{2ik_{\pi,m,n} - i\pi_{k,m,n} + q_{m,n} - i\pi_{m,n}}{(\omega_m^2 - \omega_n^2)\mu\epsilon_b} \times \left[2ik_{\pi,n,m} - i\pi_{k,n,m} + q_{n,m} - i\pi_{n,m} + (\omega_\lambda^2 - \omega_m^2)\mu\epsilon_{f,n,m}\right] \Bigg\} + \sum_{\mathbf{k}'} \omega_\lambda^2 \mu\epsilon^s_{\mathbf{k}'-\mathbf{k}} W_{\lambda,n,\mathbf{k}'} = 0. \tag{14}$$

For semiconductors the large term in braces in the equation above is used to define an effective mass which characterizes each particular region of semiconductor in a heterostructure (Chow and Koch 1999). Here we proceed in a similar fashion by defining an effective mass-like term:

$$\frac{1}{m^*} \triangleq -\sum_{m \neq n} \frac{2ik_{\pi,m,n} - i\pi_{k,m,n} + q_{m,n} - i\pi_{m,n}}{k^2(\omega_m^2 - \omega_n^2)\mu\epsilon_b} \times \left[2ik_{\pi,n,m} - i\pi_{k,n,m} + q_{n,m} - i\pi_{n,m} + (\omega_\lambda^2 - \omega_m^2)\mu\epsilon_{f,n,m}\right]. \tag{15}$$

Using this definition, we now take the Fourier transform of the wave equation, Equation (14). This is done by multiplying by $\exp(i\mathbf{k} \cdot \mathbf{R})$ and integrating over $\mathrm{d}^3\mathbf{k}$. We then employ the definition:

$$W_{\lambda,n}(\mathbf{r}) \triangleq \sum_{\mathbf{k}} \exp(i\mathbf{k}\cdot\mathbf{r})\, W_{\lambda,n,\mathbf{k}}, \tag{16}$$

to obtain the final equation:

$$\left[\frac{\nabla^2}{m^*} + \omega_\lambda^2 \mu \epsilon_s(\mathbf{R})\right] W_{\lambda,n}(\mathbf{R}) = -(\omega_\lambda^2 - \omega_n^2)\mu\epsilon_b W_{\lambda,n}(\mathbf{R}). \tag{17}$$

The above equation is very similar to the starting wave equation, Equation (2), with two important differences. First of all, the equation has no direct reference to the dielectric profile of the photonic crystal, ϵ_f. There is also no reference to the position variable ρ describing positions within the unit cells of the crystal. The only position variable used here is $\mathbf{R}$ which only describes the positions of the individual lattice cells, and is used to characterize the slower variations due to the junctions, ϵ_s. The second difference between the above equation and the starting equation is the appearance of the effective mass, m^*. This parameter contains information about the underlying photonic crystal.

Equation (17) is very similar in shape to the Schrödinger equation of a particle in a quantum mechanical system. In fact, techniques and solutions developed for quantum mechanical particles may be applied directly for its solution. As was shown successfully in (E. Istrate and E. H. Sargent, submitted), both quantum wells (Yano *et al.* 2000) and superlattices (Istrate and Sargent 2000a) can be analysed with great precision using the equations developed for the study of semiconductors (Bastard 1988).

3. Application to the study of graded junctions

The envelope approximation allows the analysis of photonic crystal junctions using a two-step approach. In the first step the effective mass is computed for all photonic crystals in the junction. This only requires knowledge of the bulk properties of the photonic crystals, which are well known. Needed in particular are the band-edge frequencies of the crystals as well as the electromagnetic modes at these edges. These parameters are used in Equation (15) to compute the effective mass. The second step is to solve the envelope Equation (17), for which again many techniques are available, both analytical and numerical. The result of this calculation is either a real-valued wave vector, indicating that waves can propagate through the structure, or a complex decay constant, describing waves in the stop-band of the structure which are rejected.

The two-step approach described above is also applicable for graded junctions. The only complication added is due to the fact that we do not have

a finite number of bulk crystals forming the junctions. Instead, the properties of the crystal vary continuously with position in the junction, which produces a continuously varying effective mass. Such an effective mass cannot be calculated directly by the method described above, since we do not have a uniform crystal from which to compute the band structure and eigenmodes required. We can solve this problem by approximating the graded crystal by a sequence of junctions between narrow, uniform layers of photonic crystals. Effective masses are computed for all of these crystals. The true effective mass profile for the graded crystal is then obtained by interpolation from this set of effective masses.

4. Example calculation

To illustrate the technique described in the previous sections, we report the analysis of a graded photonic crystal obtained by non-uniform infiltration of a high-index material. For simplicity, the method is described in one-dimension, but is fully deployable in 3D structures.

The profile of the structure is shown in Fig. 1. It is assumed that infiltration was stronger near the edges of the sample, whereas little material was infiltrated in the centre. The structure is 25 μm long with lattice period 500 nm. Its refractive index varies between 1 and 2. It is assumed that the cells near the edges are 80% full of the high-index material, while at the centre, they are 50% full. The variation in the fill ratio is assumed to vary linearly.

The structure is split into 13 slices and the envelope approximation is applied to each one. The results are tabulated in Table 1. The profile of the effective mass is shown in Fig. 2.

As a result of the varying properties of the graded junction, the band edges also move. The position of the first two $\mathbf{k} = 0$ band edges is computed and displayed in Fig. 3. The area between these two edges forms a stop band, which is indicated in this figure by the shading.

The effective mass profile, together with the shape of the band edges, give a complete description of our graded junction, enabling us to analyse the behaviour of light entering it. It is readily seen that the band gap profile in

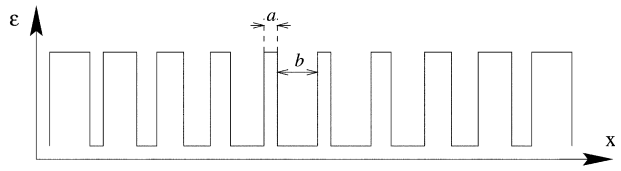

Fig. 1. Dielectric profile of example graded crystal.

Table 1. Results of the simulation

Position (μm)	a (nm)	b (nm)	m^*
0	100	400	−0.0227
2.08	125	375	−0.0293
4.17	150	350	−0.0361
6.25	175	325	−0.0429
8.33	200	300	−0.0477
10.42	225	275	−0.0532
12.5	250	250	−0.0534

Only results for the first half of the structure are shown, since the other half is symmetrical with the first.

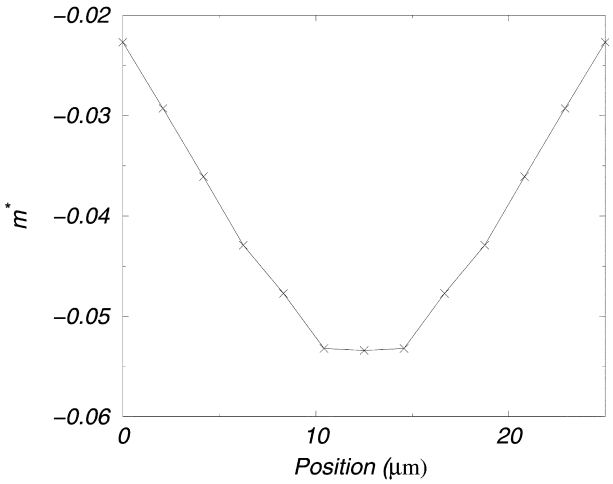

Fig. 2. Variation of the effective mass with position in the sample.

Fig. 3 forms a well that could confine light resonantly, in a manner similar to a quantum mechanical well.

The eigenstates of this photonic well are readily computed just as bound states of a semiconductor heterojunction are obtained. The equation governing the behaviour of light in this junction is obtained from Equation (17):

$$\frac{1}{m^*}\frac{\partial^2}{\partial x^2}\left[W_{\lambda,n}(x)\right] = -\left[\omega_\lambda^2 - \omega_1^2(x)\right]\mu\epsilon_b W_{\lambda,n}(x) \tag{18}$$

This equation can be solved numerically using the effective mass and band-edge profiles. For our example structure we have found a state that satisfies the boundary condition requirement of zero amplitude as $x \to \pm\infty$. Such a state was found for a wavelength of 0.859 μm. The position of the bound state and its shape are shown in Fig. 3.

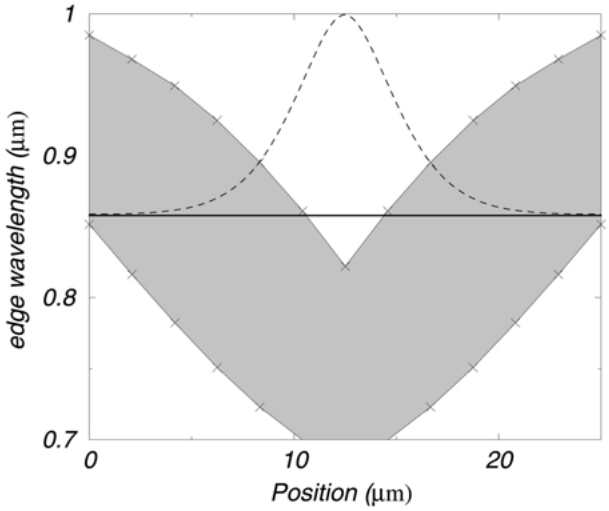

Fig. 3. Band edges and the resonant state in the sample. The shaded area represents the band gap. The thick line gives the resonant wavelength, the dashed line shows the shape of the resonant state.

5. Conclusions

The envelope approximation was shown to be an essential tool for analysing semiconductor heterojunctions. We have applied the same concept to photonic crystal graded junctions. These are crystals whose parameters vary slowly with position. This variation makes graded junctions non-periodic, which means that the standard methods for the analysis of bulk crystals cannot be applied any more.

In the method developed herein, the bulk crystals forming the junction are first used to obtain an effective mass. The photonic crystals may then be treated as quasi-homogeneous materials which are analysed using the standard methods developed for quantum mechanics.

Using this approximation, it was shown that graded photonic crystal junctions are easily analysed. In our example structure we have found the wavelength at which light will be confined resonantly in the fundamental mode of the structure.

Although graded crystals can appear naturally during the fabrication of normal crystals through infiltration or holography, they can also be fabricated in such a way as to exploit their useful properties. For this, gradings could be made by non-uniform infiltration, as above, or by sedimentation of colloidal crystals, in a way similar to the one described in (Kumacheva *et al.* 1999), by starting with a suspension of non-uniform spheres, and achieving mass-dependent order of sedimentation.

A good understanding of graded photonic crystals is essential for the engineering of functional devices based on photonic crystals. By choosing the

Fig. 4. Possible application of graded photonic crystal junctions, representing an input coupler, a resonant well and an output coupler.

correct grading profile, equally spaced states in a photonic crystal quantum well can be achieved, in a similar way to the equal spacing displayed by parabolic semiconductor quantum wells (quantum harmonic oscillators). Graded photonic crystals can also facilitate the input and output of light from photonic crystal-based devices, in a manner similar to the formation of ohmic contacts. In such a way, light could be input in a region of the crystal where propagation is permitted at the wavelength of interest. A grading in the crystal is then used to bring light into a region where the light can be influenced by the crystal. Since the grading is smooth, the transitions can be achieved without reflections due to discontinuities, as illustrated in Fig. 4. In this way, photonic crystal gradings could also be used as anti-reflection regions.

References

Bastard, G. *Wave Mechanics Applied to Semiconductor Heterostructures*. Les éditions de physique, Les Ulis, France, 1988.

Blanco, A., E. Chomski, S. Grabtchak, M. Ibisate, S. John, S.W. Leonard, C. Lopez, F. Meseguer, H. Miguez, J.P. Mondia, G.A. Ozin, O. Toader and H.M. van Driel. *Nature* **405** 437, 2000.

Campbell, M., D.N. Sharp, M.T. Harrison, R.G. Denning and A.J. Turberfield. *Nature* **404** 53, 2000.

Chow, W.W. and S.W. Koch. *Semiconductor-Laser fundamentals: Physics of the Gain Materials*. Springer, New York, 1999.

Furlan, J., F. Smole and P. Popovic. *Amorphous Silicon Technology – 1993 Symposium, Mater. Res. Soc.* 363, 1993.

Istrate, E. and E.H. Sargent. *International workshop on photonic and electromagnetic crystal structures*, p. T4, Sendai, Japan, RIEC, 2000a.

Kumacheva, E., O. Kalinina, and L. Lilge. *Adv. Mat.* **11** 231, 1999.

Li, Y.J., H.M. Shieh, J.S. Su, M.J. Kao and W.C. Hsu. *Mat. Chem. Phys.* **61** 266, 1999.

Marcinkevicius, S., U. Olin, J. Wallin and G.L.K. Strebel. *Conference on Lasers and Electro-Optics*, p. 280, 1995.

Sinkkonen, J. *1994 IEEE First World Conference on Photovoltaic Energy Conversion*, p. 26, 1994.

Weisbuch, C. and B. Vinter. *Quantum Semiconductor Structures: Fundamentals and Applications*. Academic Press, Boston, 1994.

Wuyts, K., J. Watte, R.E. Silverans, H. Muner, M.G. Berger, H. Luth, M.V. Hove and M.V. Rossum. *Advanced Metallization and Processing for Semiconductor Devices and Circuits - II. Symposium. Mater. Res. Soc.* 355, 1992.

Yano, S., Y. Segawa, J.S. Bae, K. Mizuno, H. Miyazaki, S. Yamaguchi and K. Ohtaka. *International workshop on photonic and electromagnetic crystal structures*, p. W4, Sendai, Japan, RIEC, 2000.

Yih, G.W., K. Gioney, J. Bowers, M. Rodwell, P. Silvestre, P. Thiagrajan and G. Robinson. *J. Lightwave Technol.* **13** 1490, 1995.